Conformation and Ion-Channeling Activity of a 27-Residue Peptide Modeled on the Single-Transmembrane Segment of the IsK (minK) Protein[†,‡]

Amalia Aggeli, Mark L. Bannister, Mark Bell, Neville Boden,* John B. C. Findlay, Malcolm Hunter, Peter F. Knowles, and Ji-Chun Yang[§]

Centre for Self-Organising Molecular Systems, University of Leeds, Leeds LS2 9JT, U.K.

Received August 25, 1997; Revised Manuscript Received February 26, 1998

ABSTRACT: IsK (minK) protein, in concert with another channel protein KVLQT1, mediates a distinct, slowly activating, voltage-gated potassium current across certain mammalian cell membranes. Site-directed mutational studies have led to the proposal that the single transmembrane segment of IsK participates in the pore of the potassium channel [Takumi, T. (1993) *News Physiol. Sci. 8*, 175−178]. We present functional and structural studies of a short peptide (K27) with primary structure NH_2-[1]KLEALYI-LMVLGFFGFFTLGIMLSYI[27]R-COOH, corresponding to the transmembrane segment of IsK (residues 42−68). When K27 was incorporated, at low concentrations, into phosphatidylethanolamine, black-lipid membranes, single-channel activity was observed, with no strong ion selectivity. IR measurements reveal the peptide has a predominantly helical conformation in the membrane. The atomic resolution structure of the helix has been established by high-resolution ^{1}H NMR spectroscopy studies. These studies were carried out in a solvent comprising 86% v/v 1,1,1,3,3,3-hexafluoro-isopropanol−14% v/v water, in which the IR spectrum of the peptide was found to be very similar to that observed in the bilayer. The NMR studies have established that residues 1−3 are disordered, while residues 4−27 have an α-helical conformation, the helix being looser near the termini and more stable in the central region of the molecule. The length (2.6 nm) of the hydrophobic segment of the helix, residues 7−23, matches the span of the hydrocarbon chains (2.3 ± 0.25 nm) of fully hydrated bilayers of phosphatidylcholine lipid mixture from egg yolk. The side chains on the helix surface are predominantly hydrophobic, consistent with a transmembrane location of the helix. The ion-channeling activity is believed to stem from long-lived aggregates of these helices. The aggregation is mediated by the π-π stacking of phenylalanine aromatic rings of adjacent helices and favorable interactions of the opposing aliphatic-like side chains, such as leucine and methionine, with the lipid chains of the bilayer. This mechanism is in keeping with site-directed mutational studies which suggest that the transmembrane segment of IsK is an integral part of the pore of the potassium channel and has a similar disposition to that in the peptide model system.

INTRODUCTION

IsK (or minK)[1] protein is found in the mammalian cell membranes of the epithelia, the heart, the kidney, and the uterus. In cardiac muscle cells, it is responsible, together with many other voltage-gated ion channels, for the generation of action potentials: abnormality in the functioning of these channels is associated with arrhythmic behavior (*1*).

IsK protein expression induces a slowly activating, voltage-gated potassium current across the outer membranes of *Xenopus laevis* oocytes (*2*) or mammalian HEK 293 cells (*3*, *4*). Recent experiments have shown that this current is due to the association of IsK protein with another channel protein, KVLQT1 (*5*, *6*).

IsK has no significant homology to the primary structures of other cloned potassium channels (*2*), comprising just 130 residues. This is in contrast to the Shaker channel family, which, like KVLQT1, possesses approximately 700 amino acids (*6*, *7*). IsK appears to have only a single-transmembrane segment, which places the C and N termini of the protein on the cytoplasmic and extracellular sides of the membrane, respectively, as suggested by hydropathy analysis and immunogold electron microscopy (*7*, *8*). IsK, together with a small number of other proteins such as phospholamban (*9*), influenza virus M2 (*10*), and channel-inducing factor (*11*), are examples of relatively short polypeptides with single, putative transmembrane segments, which have been speculated to be involved in ion-channeling activity.

[†] This research was supported by Grant GR/J31094 from the BBSRC Council.

[‡] The provisional entry name for K27 in the Protein Data Bank is BNL-2014.

* To whom correspondence should be addressed.

[§] Present address: MRC Laboratory of Molecular Biology, Hills Rd, Cambridge, CB2 2QH, UK.

[1] Abbreviations: $\tilde{\nu}_{max}$, maximum absorption of FTIR amide I or II; BLM, black lipid membrane; CD, circular dichroism; DMPC, 1,2-dimyristoyl-sn-glycerol-3-phosphocholine; DQFCOSY, double quantum filter correlation spectroscopy; eggPC, phosphatidylcholine lipid mixture from egg yolk; FMOC, fluorenylmethoxycarbonyl group; FTIR, Fourier transform infrared; HEK, human embryonic kidney (cell line); HFIP, 1,1,1,3,3,3-hexafluoro-isopropanol; HR ^{1}H NMR, high-resolution proton nuclear magnetic resonance; K27, peptide modeled on the transmembrane segment of IsK protein, residues 42−68; minK, minimal potassium protein; NOE, nuclear Overhauser effect; PE, phosphatidylethanolamine; PC, phosphatidylcholine; $R_{w/l}$, $R_{p/l}$, water and peptide mole ratios, respectively, relative to lipid; TFA, trifluoroacetic acid; TFE, 2,2,2-trifluoroethanol; TOCSY, total correlation spectroscopy.

S0006-2960(97)02112-0 CCC: $15.00
Published on Web 06/02/1998

Table 1: Summary of the Effects of Single-Residue Mutations in the Transmembrane Segment of IsK on the Functionality of the Potassium Channel[a]

mutants of IsK	effect of mutation on the functional properties of the potassium channel
M9(50) → L, T18(59) → V, I21(62) → L, R27(68) → Q	reduce the current of K^+ ions
F14(55) → T, F14(55) → A	diminish channel blocking activity of Cs^+ by enhancing its permeability
F14(55) → T and T18(50) → F (both mutations at the same time)	restore wild-type ionic selectivity
L11(52) → I, M22(63) → L	increase conductance
F14(55) → C, F17(58) → C	affect kinetics of voltage-gating
K1(42) → Q, E3(44) → Q, Y6(47) → F, I7(48) → L, G12(53) → C, G12(53) → A, F13(54) → C, F14(55) → L, G15(56) → C, G15(56) → A, F16(57) → C, F17(58) → L, G20(61) → A, S24(65) → A, Y25(66) → F	no effect on the ion channel properties

[a] The numbers outside the parentheses show the position of the corresponding residues in the K27 peptide chain, while the numbers inside the parentheses show the position of the corresponding residues in the IsK.

Point mutations in the single-transmembrane domain of IsK alter the gating and selectivity of the ion channel (Table 1) (*12, 13*). The selectivity changes strongly suggest that, at least, a portion of IsK lines the pore of the channel. The segment 41−90 of IsK, which encompasses the transmembrane segment and which is essential for conductance, is also the most highly conserved part of the protein. In fact the segments 41−90 of IsK from human or rat are nearly 100% homologous, apart from two changes at positions 48 (IsK_{rat}:I48 → IsK_{human}:V48) and 76 (IsK_{rat}:H76 → IsK_{human}:N76). By contrast, the segments near the N and C termini of the protein have homologies of 57% and 64%, respectively. The fact that the segment 41−90 has been preserved virtually unaltered, while the rest of the protein has suffered extensive changes, further suggests that this segment is essential for the functioning of the protein. Despite the wealth of functional studies of IsK, little is known about its precise architecture or function−structure relations.

Apart from the functional studies of IsK in vivo, there have also been reports that functional channels can be formed by truncated forms of IsK alone in vitro. Two peptides, the shortest being 32 residues long, encompassing the transmembrane segment of IsK, have been studies previously, in order to evaluate the functional role of the transmembrane domain of IsK. The 32-residue peptide was modeled on residues 41−72 (*14*), while a 63-residue peptide ("truncated IsK") was modeled on residues 1−9 linked to residues 41−94 (*15*). These peptides, when incorporated into lipid bilayers, formed conducting channels. The main source of structural information in these studies was CD spectroscopy on methanolic solutions of the peptides. The presence of 57% and 31% helical conformations was estimated for an 11 μM solution of the 32-residue peptide and for a 15 μM solution of the 63-residue peptide, respectively.

In this paper, we present the results of more extensive structural and functional studies on a shorter peptide (K27), which encompasses the transmembrane segment of IsK. The primary structure of K27 is

NH_2-^{1}KLEALYILMVLGFFGFFTLGIMLSYI^{27}R-COOH

It is the same as the segment of IsK which spans the lipid hydrophobic core, plus a few polar residues on either side (residues 42−68 of IsK). The polar residues are included to anchor the termini of the peptide chain in the lipid−water interface. The functional properties of K27 are assessed by its ability to induce single channels in planar bilayers. However, to understand the structural basis for function, it is essential to characterize both the conformation and the aggregation behavior of the peptide in the membrane. Peptides incorporated into membranes are not readily amenable to detailed analysis of their secondary structure, because X-ray crystallography and high-resolution (HR) NMR spectroscopy can not easily be applied to membrane-bound peptides. We have developed an indirect solution to this problem. First, FTIR spectroscopy is used to obtain the signature of the secondary structure of the peptide in a lipid membrane containing low peptide concentrations, prepared similarly to the ones used for the conductance studies. Second, a solvent mixture is found in which the peptide adopts a similar conformation, as indicated by its IR spectrum. Third, ^{1}H NMR is used to establish the secondary structure of the peptide in this solvent mixture. The conformation of the peptide revealed by ^{1}H NMR in solution is argued to be relevant to its conformation in the membrane. In order for this assertion to be tenable, the extramembranous segments of the peptide have been kept to a minimum, despite the fact that the predominantly hydrophobic character of such a peptide made it insoluble in most solvents and created problems in its synthesis and purification.

The NMR studies have established that residues 1−3 are disordered, while residues 4−27 have an α-helical conformation, the helix being looser near the termini and more stable in the central region of the molecule. The length (2.6 nm) of the hydrophobic segment of the helix, residues 7−23, matches the span of the hydrocarbon chains (2.3 ± 0.25 nm) of fully hydrated bilayers of phosphatidylcholine lipid mixture from egg yolk. The side chains on the helix surface are predominantly hydrophobic, consistent with a transmembrane location of the helix. The ion-channeling activity is believed to stem from long-lived aggregates of these helices. The aggregation is mediated by the π-π stacking of phenylalanine aromatic rings of adjacent helices and by favorable interactions of the opposing aliphatic-like side chains, such as leucine and methionine, with the lipid chains of the bilayer. This mechanism is in keeping with site-directed mutational studies which suggest that the transmembrane segment of IsK is an integral part of the pore of the potassium channel and has a similar disposition to that in the model peptide system.

MATERIALS AND METHODS

Peptide Synthesis and Purity. The peptide K27 was synthesized using FMOC procedures and purified as described in ref 16. Amino acid sequence analysis (Department of Biochemistry, University of Leeds) of the first six residues from the N terminus indicated >90% purity in relation to deletion peptides.

Peptide AcK27NH_2 differs from K27 in that it has acylated and amidated N and C termini, respectively. A resin, containing a linker which could be cleaved to leave the amidated form of the residue at the C terminus, was used for the synthesis of this peptide. Acylation of the N terminus was carried out prior to cleavage of the peptide from the resin, using *N*-*N*′-dicyclohexyl carbodiimide (DCC) and *N*-hydroxybenzotriazole (HOBT) dissolved in dimethylformamide (DMF) (*17*). The resin was subsequently washed with excess DMF, to remove any residual DCC and HOBT reagents, and further treated in the same way as the other peptides.

Electrospray mass spectrometry (Department of Biochemistry, University of Leeds and EPSRC Mass Spectrometry Service, University of Wales, Swansea) confirmed the dominance of peptides with the correct mass numbers for K27 (3157) and for AcK27NH_2 (3197), respectively, in the high molecular weight regions of the mass spectra. ^{19}F NMR and elemental analyses indicated the presence in the peptide of residual TFA from the synthesis, at a mole ratio of about 4 TFA/peptide; this TFA could not be removed by washing with diethylether.

In order to ensure consistency of results, all data presented here were obtained using peptide freeze-dried from solution in HFIP−H_2O (1:100 v/v), which has been shown by FTIR to have an α-helical rather than an aggregated β-sheet structure.

Conductance in Black Lipid Membranes. Black lipid membranes (BLM) were formed from egg phosphatidylethanolamine (PE)/decane at a concentration of 50 mg/mL. All lipids were purchased from Lipid Products, Redhill, Surrey, UK, and stored in sealed ampoules at −20 °C. Membranes were painted across a 150-μm aperture partitioning two solution-filled compartments. The electrolyte, 150 mM KCl, was buffered with 10 mM HEPES, and adjusted to pH 7.3 with KOH. An IDB562 membrane admittance meter (IDB, Bangor) was connected to the compartments via Ag/AgCl electrodes and agar bridges. Membrane thinning was monitored by measuring membrane capacitance. Membrane conductance was measured by voltage-clamping the cis compartment relative to the trans compartment which was held at virtual ground. Only stable bilayers with conductances <5 pS, and no intrinsic activity, were used.

Peptide ion channels were incorporated by vesicle fusion using osmotic gradients. Vacuum-dried mixtures of K27 and egg phosphatidylcholine (PC) in HFIP, $R_{p/l} = 0.0005-0.01$, were hydrated with buffered 600 mM KCl to give a lipid concentration of 5 mg/mL. After vortex mixing for a few seconds, the suspension was sonicated (Branson 250 Sonifier) for 15 min at 4 °C and under nitrogen. Vesicles were added to the stirred cis compartment which was first perfused with buffered 450 mM KCl solution. Recordings were made with 450 mM KCl, 10 mM HEPES (pH 7.3) in the cis chamber and with 150 mM KCl, 10 mM HEPES (pH 7.3) in the trans chamber, respectively, and currents were recorded at voltages ranging from +60 to −60 mV.

Raw channel data were stored on magnetic tape using a DAT recorder (DTR-1202, Bio-Logic, Grenoble). On playback, records were low-pass filtered at 50 Hz with an 8-pole Bessel filter and digitized at 2 ms/point using a Labmaster DMA and TL-1 interface with pClamp and Axotape software (Axon Instruments Inc., Foster City, CA) and an IBM-compatible computer (Elonex, UK).

Preparation of Samples for Spectroscopic Studies

1. Peptide Solutions for ^{1}H NMR. A solution of 4 mM K27 in HFIP-d_2, $(CF_3)_2$CDOD (K&K Greeff Ltd, Surrey) was used for spectral assignments, and a solution of 1.5 mM K27 in HFIP-d_1, $(CF_3)_2$CDOH was used for solving the structure of the peptide. Samples were contained in 5 mm o.d. NMR tubes. The samples were frozen in liquid nitrogen, degassed, and flame-sealed. HFIP-d_1 was obtained by mixing 5 mL of HFIP-d_2 with excess H_2O and by subsequent collection of the alcohol by distillation after several hours. FTIR and ^{1}H and ^{19}F NMR showed the presence of 14% v/v H_2O in the HFIP-d_1 fraction; this NMR samples of K27 is thus in a solvent whose composition (86% HFIP−14% H_2O) corresponds to the FTIR and CD samples (see 2 and 3 following).

2. Peptide Solutions for CD. Samples were prepared by drying down aliquots of peptide solution in hexafluoroisopropanol (HFIP) under nitrogen/vacuum to a thin film, followed by addition of a mixture of 86% v/v HFIP−14% v/v water (which is the same solvent mixture as the one used for obtaining the high-resolution ^{1}H NMR data). The solutions were mixed, placed in a bath sonicator for a few seconds, and left to equilibrate for two days at room temperature, prior to data collection. The peptide concentration was determined by amino acid analysis. Calculation of the fractional helicities was based on the observed mean residue molar ellipticity at 222 nm (*18*, *19*).

3. Peptide Solutions for FTIR. Solutions of peptide in a wide range of solvents (for example in HFIP, TFE, 2-chloroethanol, chloroform, dichloromethane, methanol, ethanol, propanol, and water) were prepared by addition of an appropriate volume of the solvent to preweighed amounts of freeze-dried peptide. After manual mixing, these samples were left at ambient temperature overnight. If the peptide had not fully dissolved, the solution was further subjected to bath sonication for 20 min and heated at 40 °C for 2 h in a tightly closed glass tube, in order to fully solubilize the peptide.

4. Peptide−Lipid Bilayers for FTIR. Peptide and egg phosphatidylcholine (average molecular weight 780 ± 7) were codissolved in HFIP, $R_{p/l} = 0.01-0.02$. The solvent was removed by solvent evaporation under a nitrogen stream followed by vacuum for 10 h until a homogeneous, dry film was obtained. D_2O or H_2O was then added to make samples of water-to-lipid mole ratio, $R_{w/l}$, between 25 and 100. The sample tube was flame-sealed to avoid loss of water by evaporation. The viscous samples were mixed by repetitive centrifugation during equilibration at room temperature for up to 2 days. The integrity of the lipid was confirmed by thin layer chromatography (TLC) on silica gel plates, using 61% v/v chloroform, 35% v/v methanol, and 4% v/v NH_3

as developing solvent. Phospholipids were detected by spraying with the reagent molybdenum blue (Sigma). The concentration of lipid was measured using the Bartlett lipid phosphate assay (*20*).

CD Spectroscopy. All CD measurements were obtained with a Jasco J-715 spectropolarimeter, using a 1 mm flat quartz cell. Spectra were recorded with 1 nm sampling intervals, at a scan rate of 50 nm/min, over the wavelength range 190−260 nm. The sensitivity was set at 50 mdeg with a response time of 1 s. Spectra were recorded over the peptide concentration range 2.5−80 μM (7.9−252.6 μg/mL, respectively). Each spectrum was an average of multiple scans. Samples with peptide concentrations of 10 μM or below were scanned 10 times, while more concentrated peptide solutions were scanned 5 times. Spectra were solvent subtracted and smoothed. The effect of temperature was investigated by data collection during cooling of the samples from 40 °C down to 0 °C at 5 °C intervals. The samples were allowed to equilibrate for 5 min at each temperature prior to data collection. Spectra collected after a 5 min or a 10 min incubation period of the samples at each temperature were found to be identical.

FTIR Spectroscopy. Spectra were recorded using a Perkin-Elmer 1760X FTIR spectrometer at 4 cm^{-1} resolution. The samples were placed between CaF_2 crystals, separated by a teflon spacer 50−100 μm thick, in a thermostated Specac liquid cell, at 20 °C. The solvent spectrum was removed by spectral subtraction. Second derivative analysis of the peptide amide I band was employed to identify the number and positions of the individual bands. The spectral areas of each of the bands were derived using home-written band-fitting software: this involved fitting the experimental bandshapes to mixed Lorenzian−Gaussian bandshape functions. The fractional areas of the component bands, assigned to different types of secondary structure, were taken to represent the proportion of the peptide chain in that structure (*21, 22*).

^{1}H NMR Spectroscopy. The experiments were carried out on a Varian Unity 500 MHz NMR spectrometer at 25 °C. A soft-pulse presaturation was applied to suppress the solvent peak. The presaturation did not affect the intensity of the amide proton signals, as the exchange between amide protons and hydroxyl protons of the solvent is fairly slow. All the two-dimensional NMR experiments were run in the phase-sensitive mode by using the hypercomplex method (*23*). Delays of 1.5 to 1.8 s were used between scans, while a 0.1 ms homospoil field was applied before the delay to reduce rapid acquisition artifacts. Typically, two-dimensional spectral data were collected with a size of 2K for t_2 and 512 t_1 increments in TOCSY and NOESY experiments (*24*). After zero-filling and Fourier transformation, the final matrices contained 2K × 1K real points. The typical data set size was 4K × 800 for DQFCOSY experiments and the transformed size, 4K × 2K points. Prior to two-dimensional Fourier transformation, the time domain data were multiplied by Gaussian window functions in both dimensions. NOESY spectra were recorded with mixing times of 50, 100, 200, and 300 ms. TOCSY spectra were recorded by using 50- and 100 ms mixing times and a Waltz-16 mixing pulse sequence. Double quantum filter COSY spectra were collected using a 32-step phase-cycling sequence in order to minimize artifacts.

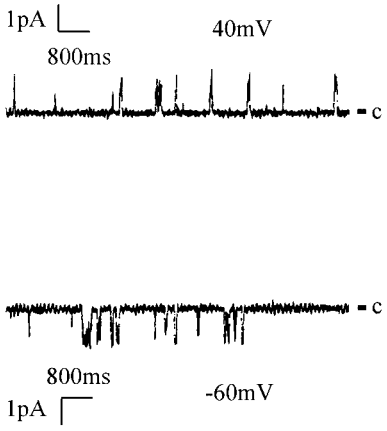

FIGURE 1: Single-channel conductance traces for K27 in PE/PC BLM. The salt (KCl) concentrations were 450 and 150 mM in the cis and trans compartments, respectively.

Molecular Modeling. Molecular modeling was carried out using the restrained molecular dynamics Biosym DISCOVER program, with the distance restraints derived from NOE cross peaks in the NOESY spectra at mixing times of 50, 100, 200, and 300 ms. The intensities of the NOEs were classified within three different levels: strong, medium, and weak. The lower and upper distance bonds were 1.5 and 3.5 Å for a strong NOE peak; 2.0 and 4.0 Å for a medium; and 2.5 and 5.0 Å for a weak peak, respectively.

RESULTS AND THEIR INTERPRETATION

Single-Channel Conductance. Figure 1 shows representative traces for K27 in a PE BLM at holding potentials of +40 and −60 mV. These traces are typically obtained after peptide incorporation in BLM by fusion of K27/eggPC vesicles containing very low peptide/lipid mole ratios ($R_{p/l}$ < 0.001).[2] Fluctuations in current due to the opening and closing of individual channels are clearly seen. In contrast, no channeling activity was observed in control experiments with lipid-only vesicles. The favored conductance states of the peptide channels were 18.5 ± 1.7 pS, 35.9 ± 1.0 pS, and 45.4 ± 1.6 pS (5 experiments). Linear I-V plots were obtained with a three-fold concentration gradient across the membrane. Voltage dependence of the channel properties was not evident: for example, the open-state probability for the channel shown in Figure 1 was 0.03 at +40 mV and 0.040 at −60 mV.

To demonstrate that the observed conductance arises largely from K27 and is not dominated by the presence of low concentrations of other peptide variants, we have compared the observed behavior with that obtained with 31- and 32-mer peptide variants. These peptides, being more polar than K27, are easier to purify by HPLC. Mass spectrometry has shown that they are indeed highly pure. At corresponding mole ratios in lipid bilayers, both of these peptides show the same channeling rate as K27, though the amplitude, lifetimes, and ion selectivity of the channels are different for the different peptides. This observation con-

[2] When K27/eggPC vesicles with significantly higher peptide concentrations were used for peptide incorporation in BLM, channels of much greater conductance (between 100 and 1500 pS) were observed. A full account of these observations will be presented in a separate publication.

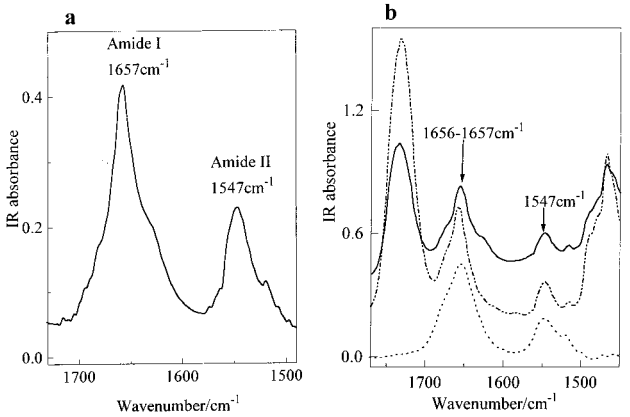

FIGURE 2: (a) IR amide I and II bands for K27 in eggPC membranes hydrated with H_2O. The contributions of H_2O and eggPC have been subtracted from the spectrum: $R_{p/l} = 0.04$, $R_{w/l} = 100$. (b) Comparison of the FTIR spectra of peptide−eggPC bilayers hydrated with D_2O: top, $AcK27NH_2$, lipid membranes, $R_{p/l} = 0.04$, $R_{w/l} = 35$; middle, K27, lipid membranes, $R_{p/l} = 0.02$, $R_{w/l} = 50$. Similar spectra are obtained with lower peptide-to-lipid mole ratio membranes. The bands at about 1730 and 1450 cm^{-1} are assigned to the lipid carbonyl stretching and lipid acyl C-H_2 scissoring vibrations respectively (*25*). The bottom spectrum is K27 in 86% v/v HFIP−14% v/v H_2O solution, peptide concentration = 5 mM.

firms that the channeling activity presented in Figure 1 is governed by K27.

Peptide Structure in eggPC Bilayers. The IR spectra of K27/eggPC bilayers with low peptide concentration ($R_{p/l} \geq 0.01$), prepared using the same procedure as for the conductance measurements, are shown in Figure 2. The position and line width of the components of the amide I and II absorption bands are diagnostic of the type and dynamics of the peptide secondary structure (*21, 22*). The position of maximum absorption, $\tilde{\nu}_{max}$, of the amide I band of K27 in eggPC bilayers hydrated with H_2O is at 1657 cm^{-1}, while $\tilde{\nu}_{max}$ of the amide II band is at 1547 cm^{-1} (Figure 2a). These features are typical of peptide in an α-helical conformation. The amide I and II bands of K27 in eggPC bilayers hydrated with D_2O are shown in Figure 2b (middle trace). It can be seen that the $\tilde{\nu}_{max}$ of both amide I and amide II are the same for peptide−lipid bilayers hydrated with either D_2O or H_2O. Other membrane proteins which are known to consist predominantly of transmembrane α-helices, including the bacterial photosynthetic reaction center from *Rhodobacterium sphaeroides*, rhodopsin (*25*), and plant photosynthetic reaction center (*26*), also have their maximum IR absorption at similar wavenumbers (1657−1656 cm^{-1}). The amide I component bands of K27 in eggPC, together with a table showing their assignments to particular types of secondary structure, are shown in Figure 3a. K27 in eggPC bilayers adopts about a 90% helical conformation. Identical results were obtained with K27−eggPC bilayers hydrated with a solution of NaCl in D_2O (NaCl/K27 mol ratio: 2/1), demonstrating that the salt, which is present in the conductance studies, does not affect the peptide secondary structure.

The similarity of the spectra of K27 (Figure 2b, middle) and $AcK27NH_2$ (Figure 2b, top) in eggPC bilayers shows that the conformation of K27 in eggPC bilayers is similar whether its N and C termini are charged or derivatized (uncharged). This is important as such charges are not present in the native protein.

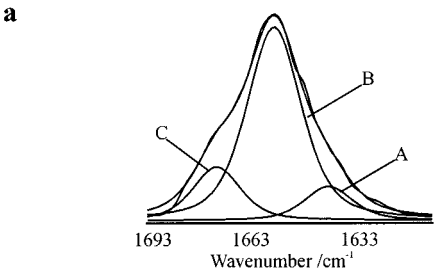

Peak /cm^{-1}	Assignment	Bandwidth /cm^{-1}	Fractional area of peak
A, 1642	random coil	16	0.09
B, 1657	α-helix	18	0.75
C, 1674	TFA	16	0.16

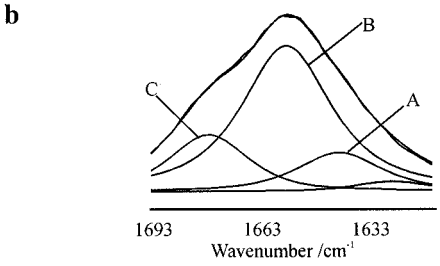

Peak /cm^{-1}	Assignment	Bandwidth /cm^{-1}	Fractional area of peak
A, 1640	random coil	28	0.14
B, 1655	α-helix	30	0.66
C, 1677	TFA	26	0.21

FIGURE 3: Comparison of the band-fitted amide I bands of (a) K27 in eggPC membranes ($R_{p/l} = 0.02$, $R_{D_2O} = 50$) and (b) of K27 in the membrane-like organic solvent 86% v/v HFIP−14% v/v H_2O, which was used for the HR ^1H NMR studies. Bands at 1674 cm^{-1} (membrane) and at 1677 cm^{-1} (solution) were assigned to TFA residual from the synthesis. The intensities and positions of these bands were also compared with control TFA solutions to ensure that they were properly assigned to TFA.

Peptide Structure in Organic Solvents

1. FTIR Studies. The self-assembly behavior of K27 in a wide range of organic solvents, particularly in alcohols and halogenated alcohols, has been investigated, in order to find an appropriate solvent for the ^1H NMR studies. It is essential that this solvent should favor the peptide secondary structure found in eggPC bilayers. The FTIR amide I and II bands of 1 mM K27 solutions in various solvents are shown in Figure 4. The conformation of K27 is seen to be very sensitive to the solvent. For example, K27 in methanol has β-sheet conformation (maximum IR absorption at 1625 cm^{-1}, bandwidth of the major band at a half height of 15−20 cm^{-1}) which induces gelation of the solution. In contrast, in solvents such as HFIP or TFE, a helical conformation or a mixture of helices and random coil conformations are obtained (maximum IR absorption at 1655 cm^{-1}, bandwidth of the major band at a half height of 25−35 cm^{-1}). An extensive account and analysis of our observations on the effects of polarity and hydrogen bonding ability of the solvent on the conformation and solubility of peptides related to K27 is presented elsewhere (*27, 28*).

The conformational propensities of K27 in organic solvents were also found to be dependent on the peptide concentration

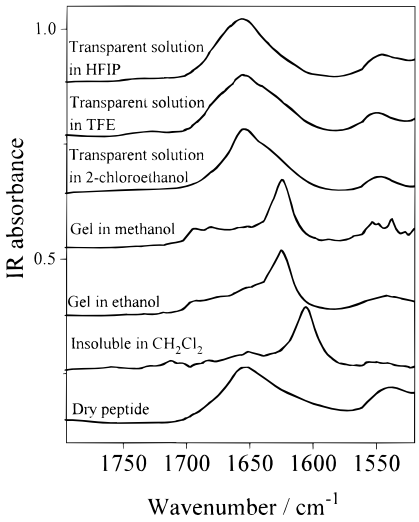

FIGURE 4: FTIR amide I and II bands of 1 mM K27 solutions in various organic solvents.

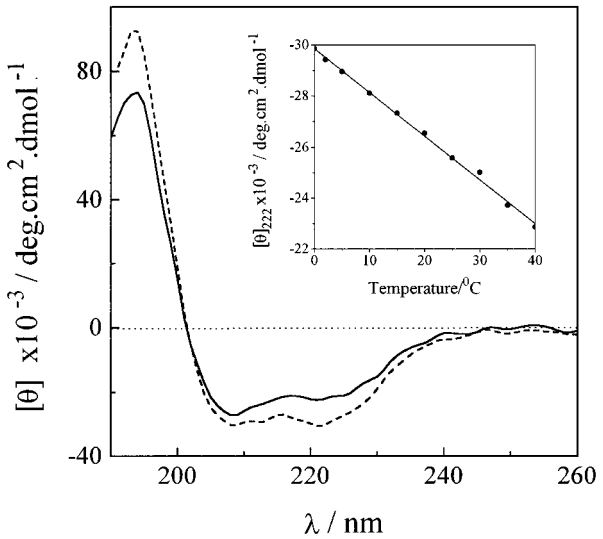

FIGURE 5: CD spectra of 5 μM K27 in 86% HFIP−14% water at 0 °C (− − −) and 40 °C (—). Insert: CD mean residue molar ellipticity at 222 nm of a 5 μM K27 solution in 86% HFIP−14% water, plotted against temperature.

in solution. For example, a conformational transition from a predominantly helical state (max IR amide I: 1655 cm^{-1}) to a predominantly antiparallel β-sheet state (max IR amide I: 1625 cm^{-1}, and weak component at 1696 cm^{-1} characteristic of antiparallel β sheet) is achieved by increasing the K27 concentration in 2-chloroethanol from 1 mM (corresponding to a fluid solution) (Figure 4) to 3 mM (corresponding to a transparent solid-like gel). In contrast, K27 solutions in HFIP with peptide concentrations at least in the range 0.5−10 mM have produced similar IR spectra, irrespective of concentration, characterized by a broad amide I band (Figure 4). The broadness of these spectra reflects a degree of instability of the secondary structure and an equilibrium between helical and random coil conformations in HFIP.

In order to diminish the disordering effect of HFIP on the peptide secondary structure, mixtures of HFIP/CH_2Cl_2 were also tried, but it was found that such mixtures do not favor the conformation of the membrane-bound state of the peptide (data not shown). This was demonstrated by the presence of a distinct IR band centered at 1610 cm^{-1} [usually assigned to another type of extended structure (*29*)], whose intensity increased by increasing the volume fraction of CH_2Cl_2 in the mixed solvent. Such a band is absent from IR spectra obtained with peptide−lipid membranes.

The second criterion for the selection of the appropriate solvent for the ^{1}H NMR studies is that it should be a "good solvent" for the peptide, in order to obtain reasonably narrow line widths and adequate signal sensitivity. This is not a trivial requirement, because the amphiphilic character of the K27 peptide (i.e., a long apolar segment between two short polar ones) makes it prone to self-aggregation in most solvents. A number of membrane peptides, which are more polar than K27 or contain special helix-stabilizing amino acid residues, have previously been found to be sufficiently soluble in methanol for NMR studies. For example, NMR studies of several transmembrane ion channel forming peptides such as alamethicin (*30*), δ-haemolysin (*31*), melittin (*32*), and a peptide based on the putative S2 membrane spanning segment of the Ca^{2+} channel of skeletal muscle (*33*) have all been carried out in methanol solutions. The highly hydrophobic c subunit of the F_o portion of the F_1F_o ATPase (*34*) and peptides derived from bacteriorhodopsin (*35*) have been successfully studied in chloroform−methanol and chloroform−methanol−$LiClO_4$ solutions, respectively. However, K27 aggregates into extensive β-sheet structures in these solvents (*27, 28*). We have found a mixture of HFIP−H_2O (86% v/v HFIP−14% v/v H_2O) to be the most appropriate solvent for ^{1}H NMR studies. The FTIR amide I band of K27 is narrower in this mixed solvent than in pure HFIP, which indicates that the presence of water diminishes the destabilizing effect of HFIP on the peptide secondary structure. A comparison of the FTIR amide I and II bands in the membrane and in the HFIP−H_2O mixture is shown in Figure 2b (middle and lower traces), while the principal components of the amide I band are compared in Figure 3.

2. Circular Dichroism. Far-UV CD study of K27 conformation in the 86% HFIP−14% H_2O mixture was carried out over a wide range of peptide concentrations from 2.5 up to 80 μM K27. Signals diagnostic of α-helical conformation were observed in all spectra, with characteristic minima of mean residue molar ellipticity at 208/222 nm and a positive maximum at 194 nm. The magnitude of the mean residue molar ellipticity at 222 nm (indicative of the fractional helicity in solution) was found to be independent of peptide concentration: $[\theta]_{222nm} = -25\,000 \pm 5000$ deg·cm^2·$dmol^{-1}$. The error margins were calculated from the uncertainty in the quantitative analysis of the peptide concentration in the solution.

The effect of temperature on the stabilities of the helices in 5, 15, and 44 μM K27 solutions was also compared. Figure 5 (insert) shows the decrease of the mean residue molar ellipticity at 222 nm as a function of temperature for a 5 μM K27 solution. Straight lines with similar slopes (within ±10%) were also obtained with 15 and 44 μM K27 solutions. The fraction of peptide in helical conformation is estimated to be 80% for both the 5 and the 44 μM samples at 0 °C, while it falls to 70% at 25 °C and to 60% at 40 °C.

3. ^{1}H NMR and Molecular Modeling. Although the line widths of the ^{1}H resonances of K27 in the HFIP−H_2O mixture are significantly broader than for a water-soluble peptide of similar size, it is still possible to follow the

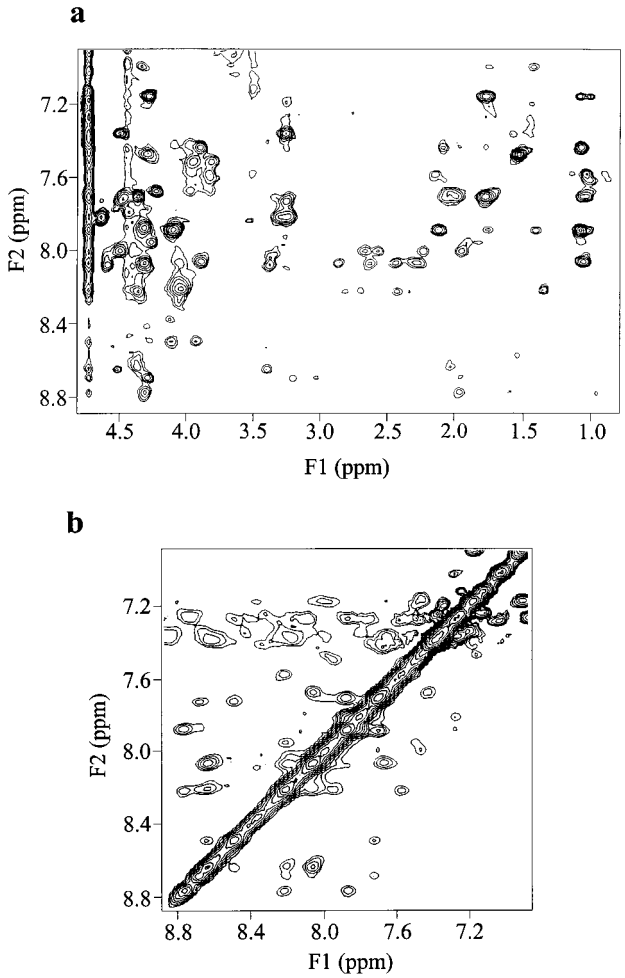

FIGURE 6: (a) TOCSY spectrum of the NH (t_2)-C$^\alpha$H and aliphatic region (t_1). The cross peaks arise from direct and relayed through-bond connectivities. (b) NOESY spectrum of the NH (t_2)-NH (t_1) region.

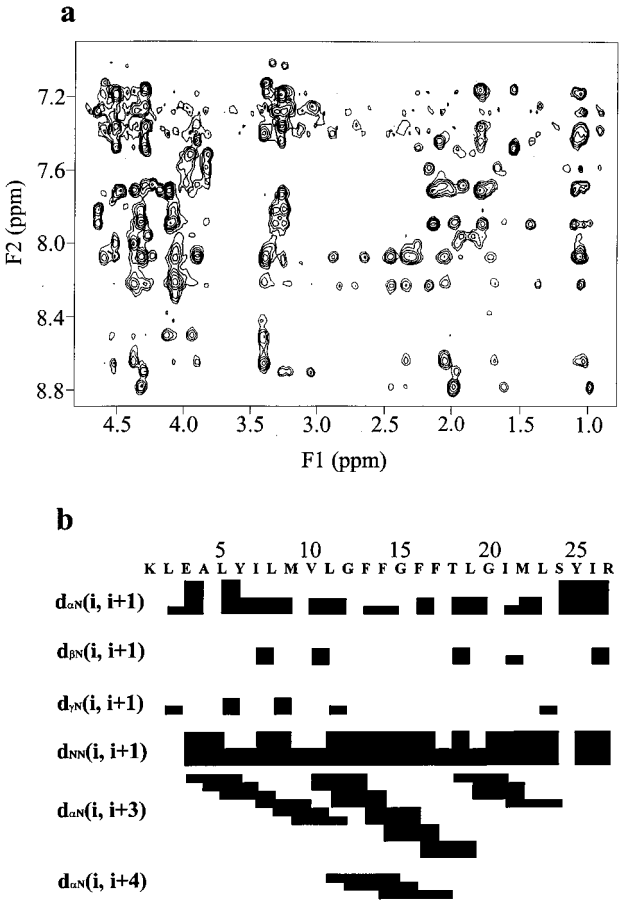

FIGURE 7: (a) NOESY spectrum of the NH (t_2)-C$^\alpha$H and aliphatic (t_1) region of K27 in solution at 25 °C. The cross peaks arise from through-space (<5.4 Å) connectivities. The distance between particular protons can be deduced by the intensity of their NOE crosspeaks. (b) Summary of NOEs classified into strong, medium, and weak, as indicated by the thickness of the lines. For interpretation of these results, see the Results section ("^{1}H NMR and molecular modeling").

connectivity along the entire molecule with the combination of TOCSY and NOESY spectra (*24*). Examples of the TOCSY and NOESY spectra are shown in Figure 6a,b and Figure 7a. A full list of the assignments is given in the Supporting Information section. The spectra are consistent with the amino acid composition of K27 peptide.

NOEs involving the NH, C$^\alpha$H, and C$^\beta$H provided the basis for a qualitative interpretation of the secondary structure. Since the first two residues do not have any NOE connectivity with other residues, they must be structurally very flexible or disordered in the solution. The appearance of the stretches of NH(i)−NH(i + 1) NOEs and the presence of C$^\alpha$H(i)−NH(i + 3) and C$^\beta$H(i)−NH(i + 3) NOEs indicate that there is a helical structure from residue 3 to residue 27. However, there are clear deviations in the NOE pattern from that of a standard helical structure. In a standard helical structure, NOEs between NH(i) and NH(i + 1) would be very strong and NOEs between C$^\alpha$H(i) and NH(i + 3) would be more intense than that of C$^\alpha$H(i)−NH(i + 1). The presence of the medium strength NH(i)−NH(i + 1) NOEs and mostly weak C$^\alpha$H(i)−NH(i + 3) NOEs between residues 3−10 and residues 20−27 of the K27 indicates the presence of some dynamic variability, suggesting that the helical conformations of these regions are less rigid than a standard helix. The presence of strong NH(i)−NH(i + 1) and medium C$^\alpha$H(i)−NH(i + 3) NOEs between residues 11−19 shows that this part of K27 has a more rigid helical conformation (Figure 7b).

The starting structure for the molecular modeling was a standard right-handed α helix of residues 3−27 with a random coil structure for the first two residues. Initially, the structure was energy-minimized for 100 steps using the steepest descents. A set of structures was collected at 5 ps intervals during a molecular dynamics run of 40 ps at 300 K, and final energy minimization on these structures was performed (Figure 8a).

DISCUSSION

Secondary Structure of K27 in Lipid Bilayers. Previous studies have established that K27 in eggPC or DMPC bilayers, prepared by dialysis of a solution of peptide/lipid in 2-chloroethanol, has a highly aggregated transmembrane β-sheet structure (*16, 36*). By contrast, we show here that K27 in eggPC bilayers with low peptide concentration (typically $R_{p/l} \leq 0.01$), prepared by evaporation of K27/eggPC solution in HFIP and subsequent hydration of the dry peptide/lipid film, adopts almost exclusively a helical conformation. This procedure of membrane reconstitution

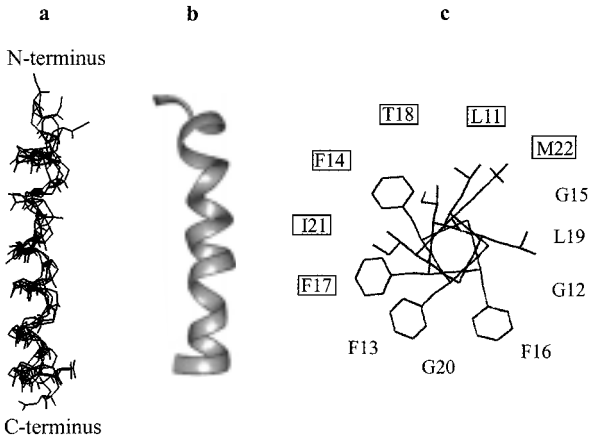

FIGURE 8: NMR-derived structure of K27 in 86% v/v HFIP−14% v/v H_2O, produced with Insight II. (a) Superposition of the peptide backbones of four calculated structures of K27. Each structure was obtained at different intervals during the 40 ps molecular dynamics run of the peptide. Molecular dynamics modeling was performed with the Biosym Discover program, taking into consideration the NOE distance constraints. (b) Ribbon representation of the backbone of one of the low-energy structures of K27. (c) Helical wheel of the segment Leu11-Met22 of K27. Boxes around labels indicate residues whose replacement with other residues changes the functionality of IsK. The absence of boxes around labels indicates residues whose replacement with other residues does not change the functionality of IsK (Table 1). The corresponding side chains of residues G12 and G15 on the IsK protein face the lipid acyl chains.

has recently been used in a study of the dependence of the peptide conformation on its concentration in the membrane (*37*).

Clearly, the conformation of K27 in a lipid bilayer is dependent on the methods of peptide incorporation. In particular, we propose that the increasing polarity of the medium, which changes from 2-chloroethanol to water during dialysis, induces self-aggregation of the predominantly apolar peptide molecules prior to or during their incorporation into the bilayers. In this way, aggregated β structures end up in the bilayer. We have observed similar behavior with the M2δ peptide, which corresponds to a transmembrane segment of Torpedo acetylcholine receptor (*38*). Incorporation of M2δ in eggPC bilayers by dialysis of a peptide/lipid solution in 2-chloroethanol resulted also in peptide self-aggregation and formation of β structures with a maximum absorbance of the FTIR amide I band at about 1622 cm^{-1}. Nonetheless, M2δ is known to adopt a helical conformation in its functional state in the membrane, where it lines the transmembrane ion channel pore of the acetylcholine receptor as shown by the cryoelectron microscopy studies of Unwin, 1995 (*38*). Thus, we conclude that, while there are known examples of proteins, such as porins (*39*), which adopt β-sheet structure in their functional state in the membrane, the β structures of highly apolar peptides, such as K27 in lipid membranes prepared by dialysis, are unlikely to be biologically relevant, but rather artifacts of the preparation procedure.

In the present study, both the single-channel conductance measurements and the peptide structural studies by FTIR spectroscopy were carried out using K27/eggPC bilayers prepared in a similar way (see Materials and Methods) which preserves the helical conformation of the peptide. This leads us to conclude that the secondary structure of the functional state of the peptide monitored by the conductance measurements is the helical one observed by FTIR.

High-Resolution Secondary Structure of K27 in Solution. The FTIR data alone demonstrate the prevalence of the helical conformation of K27 in lipid bilayers. It is well-known though that small variations in the stability of transmembrane, pore-lining helices can affect or determine their channeling mechanism. For example, there are rigid membrane-spanning helices or kinked ones (i.e., with some flexibility in the middle of the transmembrane segment). Thus the use of high-resolution NMR enables us to get detailed information on the conformation of the transmembrane segment of IsK, which is necessary in order to rationalize its functional properties.

A mixture of 86% v/v HFIP−14% v/v H_2O was selected for ^1H NMR conformational studies of the peptide, on the basis of the ability of this solvent medium to stabilize a conformation similar to its membrane-bound state, as judged by FTIR. Mixtures of HFIP−H_2O have previously been used to mimic a membrane-like environment for NMR structural studies of the antibacterial transmembrane peptide, cecropin A (*40*). Another similar mixture consisting of TFE−H_2O has also been used as a membrane-mimetic medium for the NMR structural study of the S4 segment from the Na^+ channel protein (*41*).

The NMR results for K27 show that the whole peptide chain, apart from residues 1−3, folds into a helix whose stability varies along the molecule (Figure 8b). In particular, the helical conformation of the segments 3−10 and 20−27 is not a rigid one and averaging of several conformations on the NMR timescale is likely to occur. The middle of the molecule, that is, segment 11−19, which encompasses the four phenylalanines of the primary structure, has a rigid helical conformation. It is interesting to note that the NMR-derived structure of K27 is significantly different from the results obtained with secondary structure prediction software [the software combines the results of a collection of general standard and published prediction programs based on the conformational propensities of proteins in water (*42*)]. In particular, it was predicted that the only potentially helical region is between residue 1 and residue 10, while the NMR results showed that this segment has in fact a less-stable helical conformation than segment 11−19. This difference between experiment and prediction reveals that different environments can have important effects on the peptide self-assembly.

Peptides which self-assemble into bundles of helices in solution have previously been shown to exhibit a decrease in their fractional helicities as peptide concentration is reduced (*43*). In contrast, monomeric helical peptides have been found to have the same fractional helicity over a wide range of peptide concentrations (*44*). Our CD spectroscopic studies have established that, for K27 in 86% v/v HFIP−14% v/v H_2O, the fractional helicity as well as the temperature stability of the helices is the same over a wide range of peptide concentrations (2.5−80 μM). This strongly suggests that K27 helices in 86% v/v HFIP−14% v/v H_2O are in a predominantly monomeric state.

The NMR experiments have shown that 93% of the peptide chain adopts a helical conformation (taking into account both stable and loose helical segments) in 86% v/v HFIP−14% v/v H_2O. This compares favorably with the

FTIR results which suggested a fractional helicity of 84% for the peptide in this solvent mixture. The broad FTIR component bands also suggest an overall loose helical structure for the peptide, in agreement with the NMR results. CD studies at a peptide concentration of 80 μM, which is lower than the one used in the NMR studies (ca. 1.5 mM), suggest the presence of 70% helical conformers. The differences of fractional helicities obtained from the different spectroscopic techniques [93% (NMR), 84% (FTIR), and 70% (CD)] reflect differences in averaging, stemming from the different intrinsic timescales associated with the different techniques.

Structure and Function of K27 Channels in Lipid Bilayers. FTIR has shown that 90% of the peptide has a helical conformation in the membrane, while 10% is in a random coil conformation. This is to be compared with 93% of helical conformation and 7% of random coil found by NMR. Thus, to a first approximation, it seems reasonable to take the NMR-derived conformation as a representation of the actual structure of K27 in the bilayer, and it reveals that K27 has an irregular conformation between residue 1 and residue 3, while it adopts a helical conformation for residues 3−27, the helix being looser near the termini than in the middle of the molecule. The side chains on the helix surface are predominantly hydrophobic, with polar residues mainly near the termini.

The length of the K27 helix $L_{\text{helix3-27}}$ and the length of the hydrophobic segment of the helix $L_{\text{helix4-26}}$ (i.e., excluding the charged residues at positions 3 and 27) were estimated to be 36 and 33 Å, respectively, assuming that the separation between adjacent residues along the long axis of the α helix is 1.5 Å (*45*). It is clear that the length of the helix in K27 (36 Å) matches the thickness (38 ± 2.5 Å) of eggPC bilayers at excess hydration (*46*). K27 has three charged groups near the N terminus and two charged groups near the C terminus. A transmembrane location of the K27 helix would allow the charged groups near the peptide termini to interact favorably with the polar lipid headgroups and water, while the rest of the peptide molecule, which is predominantly hydrophobic, would be embedded in the lipid hydrocarbon core.

If the peptide was outside the membrane, it would be exposed to water and consequently it would adopt a β-sheet conformation (*27*). That the K27 helices have a transmembrane location is also supported by the observation that the maximum absorbance of the FTIR amide I band of K27 in bilayers hydrated with H_2O or D_2O is at the same wavenumber, that is, at 1657 cm^{-1}. If substantial NH ⟹ ND exchange had taken place at the helical peptide backbone, a shift of the amide I maximum to a lower wavenumber by 5−10 cm^{-1} would have been observed for peptide in membranes hydrated with D_2O (*47*). K27 also preserves a strong amide II band, even after 48 h, in bilayers hydrated with D_2O. This is an unusually long time for helices exposed to D_2O, which suggests that the helix is not exposed to water and must span the lipid hydrophobic core. ATR IR on oriented peptide/lipid bilayers has demonstrated that the helices have a transmembrane orientation (Boden, N. et al., unpublished data).

The single-channel activity observed when K27 was incorporated into PE BLM, at low peptide concentrations, is as shown in Figure 1. The unitary current steps between open and closed states are characteristic of ion channels (*48*). Following insertion of channels from the vesicles into the membrane, channel activity is seen to be reasonably constant with time. Since the peptide concentration is far higher in the vesicles than in the BLM (the surface area ratio of the bilayer in BLM to that in vesicles is greater than 10^9), it follows that, once formed, channel assemblies are stable. Otherwise channel activity would be expected to decline with time as peptides diffused away from the channeling aggregates into the bulk of BLM. These channels must be bundles of α-helices.

The FTIR amide I band of the peptide in 86% HFIP−14% H_2O is broader than the corresponding bands in the lipid bilayer. This indicates that the lipid membrane stabilizes the α-helix more effectively than the solvent. This could be due to the enhancement of the stability of the helix in the bilayer environment, and also due to its presence in the relatively long-lived channeling aggregates. The aggregation of peptides in the bilayer can be contrasted with their behavior in 86% v/v HFIP−14% v/v H_2O, where peptides are in their monomeric state. The fact that the helices are not amphiphilic in the classical sense, that is, they do not possess opposing polar and apolar sides, raises the interesting question as to the nature of the attractive forces which lead to aggregation in the bilayer. Viewing the K27 helical model from the top (Figure 8c) reveals an interesting property of this structure, namely that all phenylalanine side chains are clustered on one side of the helix, with leucine, methionine, and glycine side-chains on the opposite side. Indeed, it is well-known that interactions between aromatic residues can contribute to the stabilization of the tertiary structure of proteins (*49, 50*). Thus, it is quite possible that π-π stacking of the aromatic rings of adjacent helices is a major contributor to their aggregation. Furthermore, this arrangement places the aliphatic-like side chains on the opposite side of the helix (such as leucines), in contact with the aliphatic lipid chains, which is also energetically favorable. Thus, the pore of the K27 channel has a predominantly hydrophobic character (lined by phenylalanines, isoleucines, and the single polar residue threonine 18) (Figure 8c), as opposed to the familiar model of a transmembrane polar pore formed in the middle of a bundle of amphiphilic helices (*51, 52*). The presence of hydrophobic residues, in particular aromatics, in other ion channels has been proposed by other workers (*53, 54*).

The attractive forces between helix dipoles will favor an antiparallel arrangement of helices (*55*). The net positive charge near the N terminus will also help stabilize this structure, though the effect is not expected to be too significant, because it resides in the random coil segment which is solvated by water.

Implications of the Behavior of K27 for the Structure and Function of IsK. The conductance values of K27 channels are of the same order of magnitude as those reported by Ben-Efraim et al. for a 32-mer (*14*) and a 63-mer (*15*) peptide based on the IsK transmembrane domain. Recent experiments have shown that IsK coexpresses with other channel proteins (KVLQT1 and HERG) to elicit functional channel activity (*56*). The single-channel properties of the HERG-IsK heteromeric assemblies were not different from those of HERG alone, whereas the single-channel characteristics of IsK-KVLQT1 have not yet been determined. Estimates of single-channel conductance for IsK/KVLQT1, derived by

fluctuation analysis, are of the order of fS (*57*).

In contrast to the 32-mer (*14*), with K27 we could not detect any pronounced voltage dependence of channel activity. In the 32-mer, there is an additional Ser at the N terminus and a Ser-Lys-Lys-Leu extension at the C terminus. Thus, the additional residues, probably the positively charged lysines, are likely to confer the voltage dependence on the resulting channel. Unlike IsK, neither K27 nor the 32-mer peptide is particularly ion-selective, which suggests that the selectivity filter lies outside the transmembrane segment. This may be supported by the fact that point mutations of phenylalanine 55, which lies in the middle of the putative membrane-spanning segment of IsK, yielded channels which were still highly K^+ selective (*13*).

The self-assembly of IsK in vivo is such that glycines 53 and 56 are in contact with the lipid chains in the cell membrane, while phenylalanines 54, 55, 57, and 58 are not (*58*). From the model of the helical K27 structure, it becomes clear that the corresponding glycines 12 and 15 of K27 are indeed on the same side of the helix, while the corresponding phenylalanines 13, 14, 16, and 17 are on its opposite side, in keeping with the functional results obtained with IsK. Furthermore, most single-residue mutations which affect the functional properties of the potassium channel (Table 1) lie on one side of the K27 helix (Figure 8c). For example, single-residue substitutions of threonine 59 and phenylalanine 55 on IsK have been shown to affect, respectively, the conductance of potassium ions and the Cs^+ selectivity of this channel (*12*). This evidence suggests that these side chains line the channel pore in vivo, in agreement with our model of the K27 ion pore. On the basis of the above comparison, it can be concluded that K27 peptide has the same secondary structure, the same location with respect to the membrane, and the same orientation with respect to the ion pore as those of the corresponding segment of the IsK protein, even in the absence of the rest of the IsK chain and in the absence of the other proteins, including KVLQT1, in the cell membrane.

It is therefore reasonable to suggest that the segment of IsK, which crosses the hydrocarbon core of the cell membrane, adopts a rigid α-helical conformation, similar to the nonvoltage-gated, channel-forming transmembrane domain of the amphiphilic peptide δ-haemolysin (*31*). The available experimental evidence does not suggest any propensity of the transmembrane segment of IsK to form a "kinked" helix, like the ones present in the channel-lining transmembrane segment of the acetylcholine receptor (*38*) and in two voltage-gated, channel-forming transmembrane peptides alamethicin (*30*) and melittin (*32*). The differences in the flexibilities of the transmembrane domains of these peptides and proteins could give rise to differences in their gating mechanisms.

The presence of a random coil conformation, followed by the loose helical segment near the N terminus, suggests that the segment of IsK which precedes the transmembrane one may also have an irregular conformation. Single-residue substitutions at the region which immediately precedes the membrane-spanning segment of IsK have no effect on the functional properties of the protein. For example, replacement of glutamic 44, which is located just before the transmembrane segment, with glutamine has no effect on the potassium current. If the region of IsK which immediately precedes the transmembrane segment does indeed have an irregular conformation, it could explain the lack of involvement of the side chains in this region with ion transport. By contrast, several single-residue substitutions in the segment immediately following the transmembrane segment result in altered ion currents, which indicates that this segment plays an important role in the functionality of the protein. Thus, we believe that studies similar to the one presented here in organic solvents or in surfactant micelles, for peptides including in their primary structures the segments of IsK which precede and follow the transmembrane segment, will help throw further light on the ion-channeling mechanism of IsK in vivo.

ACKNOWLEDGMENT

We thank Dr. J. Keen for assistance with peptide synthesis and quality control, Drs. Y. Cheng, A. P. Kalverda, and P. J. H. Turnbull for helpful discussions, and Dr. S. E. Radford for use of the CD spectrometer purchased with a grant from the Wellcome Trust. We also wish to thank British Telecom plc and the Engineering and Physical Sciences Research Council for financial support.

SUPPORTING INFORMATION AVAILABLE

A table of the assignments of the proton NMR resonances of K27 in the HFIP−H_2O mixture (1 page). Ordering information is given on any current masthead page.

REFERENCES

1. Attali, B. (1996) *Nature 384*, 24−25.
2. Takumi, T., Ohkubo, H., and Nakanishi, S. (1988) *Science 242*, 1042−1045.
3. Freeman, L. C., and Kass, R. S. (1993) *Circ. Res. 73* (5), 968−973.
4. Takumi, T. (1993) *News Physiol. Sci. 8*, 175−178.
5. Barhanin, J., Lesage, F., Guillemare, E., Fink, M., Lazdunski, M., and Romey, G. (1996) *Nature 384*, 78−80.
6. Sanguinetti, M. C., Curran, M. E., Zou, A., Shen, J., Spector, P. S., Atkinson, D. L., and Keating, M. T. (1996) *Nature 384*, 80−83.
7. Sugimoto, T., Tanabe, Y., Shigemoto, R., Iwai, M., Takumi, T., Ohkubo, H., and Nakanishi, S. (1990) *J. Membr. Biol. 113*, 39−47.
8. Sakagami, M., Fukazawa, K., Matsunaga, T., Fujita, H., Mori, N., Takumi, T., Ohkubo, H., and Nakanishi, S. (1991) *Hear. Res. 56*, 168−172.
9. Moorman, J. R., Palmer, C. J., John, J., Durieux, M. E., and Jones, L. R. (1992) *J. Biol. Chem. 267*, 14551−14554.
10. Pinto, L. H., Holsinger, L. J., and Lamb, R. A. (1992) *Cell 69*, 517−528.
11. Attali, B., Latter, H., Rachamin, N., and Garty, H. (1995) *Proc. Natl. Acad. Sci. U.S.A. 92*, 6092−6096.
12. Takumi, T., Moriyoshi, K., Aramori, I., Ishii, T., Oiki, S., Okada, Y., Ohkubo, H., and Nakanishi, S. (1991) *J. Biol. Chem. 266*, 22191−22198.
13. Goldstein, S. A. N., and Miller, C. (1991) *Neuron 7*, 403−408.
14. Ben-Efraim, I., Bach, D., and Shai, Y. (1993) *Biochemistry 32*, 2371−2377.
15. Ben-Efraim, I., Strahilevitz, J., and Shai, Y. (1994) *Biochemistry 33*, 6966−6973.
16. Horvath, L. I., Heimburg, T., Kovachev, P., Findlay, J. B. C., Hideg, K., and Marsh, D. (1995) *Biochemistry 34*, 3893−3898.
17. Molle, G., Dugast, J. Y., Duclohier, H., Daumas, P., Heitz, F., and Spach, G. (1988) *Biophys. J. 53*, 193−203.
18. Chen, Y., Yang, J. T., and Chau, K. H. (1974) *Biochemistry 13*, 3350.

19. Wu, C. S., Ikeda, K., and Yang, J. T. (1981) *Biochemistry 20*, 566−570.
20. Bartlett, G. R. (1959) *J. Biol. Chem. 234*, 466−468.
21. Krimm, S., and Bandekar, J. (1986) *Adv. Protein Chem. 38*, 181−354.
22. Surewicz, W. K., and Mantsch, H. H. (1988) *Biochim. Biophys. Acta 952*, 115−130.
23. Keeler, J., and Neuhaus, D. (1985) *J. Magn. Reson. 63*, 454−472.
24. Wuthrich, K. (1986) *NMR of Proteins and Nucleic Acids*, Wiley, New York.
25. Jackson, M., Haris, P. I., and Chapman, D. (1989) *J. Mol. Struct. 214*, 329−355.
26. He, W. Z., Newell, W. R., Haris, P. I., Chapman, D., and Barber, J. (1991) *Biochemistry 30*, 4552−4559.
27. Aggeli, A., Bell, M., Boden, N., Keen, J. N., Knowles, P. F., McLeish, T. C. B., Pitkeathly, M., and Radford, S. E. (1997) *Nature 386*, 259−262.
28. Aggeli, A., Bell, M., Boden, N., Keen, J., McLeish, T. C. B., Nyrkova, I., Radford, S. E., and Semenov, A. (1997) *J. Mater. Chem. 7* (7), (Special Issue on Molecular Assemblies and Nanochemistry), 1135−1145.
29. Surewicz, W. K., Leddy, J. J., and Mantch, H. H. (1990) *Biochemistry 29*, 8106−8111.
30. Esposito, G., Carver, J. A., Boyd, J., and Campbell, I. D. (1987) *Biochemistry 26*, 1043−1050.
31. Tappin, M. J., Pastore, A., Norton, R. S., Freer, J. H., and Campbell, I. D. (1988) *Biochemistry 27*, 1643−1647.
32. Bazzo, R., Tappin, M. J., Pastore, A., Harvey, T. S., Carver, J. A., and Campbell, I. D. (1988) *Eur. J. Biochem. 173*, 139−146.
33. Reid, D. G., MacLachlan, L. K., Salter, C. J., Saunders, M. J., Jane, S. D., Lee, A. G., Tremeer, E. J., and Salisbury, S. A. (1992) *Biochim. Biophys. Acta 1106*, 264−272.
34. Moody, M. F., Jones, P. T., Carver, J. A., and Campbell, I. D. (1987) *J. Mol. Biol. 193*, 759−774.
35. Sobol, A. G., Arseniev, A. S., Abdulaeva, G. V., Musina, L. Y., and Bystrov, V. F. (1992) *J. Biomol. NMR 2*, 161−171.
36. Aggeli, A., Boden, N., Cheng, Y.-L., Horvarth, L., Findlay, J. B. C., Knowles, P. F., Kovatchev, P., Marsh, D., and Turnbull, P. J. H. (1996) *Biochemistry 35*, 16213−16221.
37. Boden, N., Cheng, Y., and Knowles, P. F. (1997) *Biophys. Chem. 65*, 205−210.
38. Unwin, N. (1995) *Nature 373*, 37−43.
39. Weiss, M. S., Abele, U., Weckesser, J., Welte, W., and Schiltz, G. E. (1991) *Science 254*, 1627−1630.
40. Holak, T. A., Engstrom, A., Kraulis, P. J., Lindeberg, G., Bennich, H., Alwyn, T., Gronenborn, A. M., and Clore, G. M. (1988) *Biochemistry 27*, 7620−7629.
41. Mulvey, D., King, G. F., Cooke, R. M., Doak, D. G., Harvey, T. S., and Campbell, I. D. (1989) *FEBS Lett. 257*, 113−117.
42. Eliopoulos, E., Geddes, A. J., Brett, M., Pappin, D. J. C., and Findlay, J. B. C. (1982) *Int. J. Biol. Macromol. 4*, 263−268.
43. DeGrado, W. F., and Lear, J. D. (1985) *J. Am. Chem. Soc. 107*, 7684−7689.
44. Diaz, H., Tsang, K. Y., Choo, D., Espina, J. R., and Kelly, J. W. (1993) *J. Am. Chem. Soc. 115*, 3790−3791.
45. Creighton, T. E. (1993) *Proteins: Structures and molecular properties*, 2nd ed., Freeman, WH and Co, New York.
46. Small, D. (1986) *Handbook of Lipid Research*, Vol. 4, Plenum Press, New York and London.
47. Haris, P. I., and Chapman, D. (1995) *Biopolymers 37*, 251−263.
48. Hille, B. (1992) *Ionic Channels of Excitable Membranes*, 2nd ed., Sinauer Associates Inc, Massachusetts.
49. Burley, S. K., and Petsko, G. A. (1985) *Science 229*, 23−28.
50. Fasman, G. D. (1989) *Prediction of protein structure and the principles of protein conformation*, Plenum Press, New York.
51. Sansom, M. S. P., Kerr, I. D., and Mellor, I. R. (1991) *Eur. Biophys. J. 20*, 229−240.
52. Sansom, M. S. P. (1991) *Prog. Biophys. Mol. Biol. 55*, 139−235.
53. Kumpf, R. A., and Dougherty, D. A. (1993) *Science 261*, 1708−1710.
54. Adams, P. D., Arkin, I. T., Engelman, D. M., and Brunger, A. T. (1995) *Nat. Struct. Biol. 2*, 154−162.
55. Sheridan, R. P., Levy, R. M., and Salemme, F. R. (1982) *Proc. Natl. Acad. Sci. U.S.A. 79*, 4545−4549.
56. McDonald, T. V., Yu, Z., Ming, Z., Palma, E., Meyers, M. B., Wang, K., Goldstein, S. A. N., and Fishman, G. I. (1997) *Nature 388*, 289−292.
57. Yang, Y., and Sigworth, F. J. (1995) *Biophys. J. 68*, A22.
58. Wilson, G. G., Sivaprasadarao, A., Findlay, J. B. C., and Wray, D. (1994) *FEBS Lett. 353*, 251−254.

BI972112H